

## An Unusual 3D Coordination Polymer Based on Bridging Interactions of the Nucleobase Adenine

Juan P. García-Terán, Oscar Castillo,\* Antonio Luque,\* Urko García-Couceiro, Pascual Román, and Luis Lezama

Departamento de Química Inorgánica, Facultad de Ciencia y Tecnología, Universidad del País Vasco, Apartado 644, E-48080 Bilbao, Spain

Received April 14, 2004

The first 3D coordination polymer containing a nucleobase as a bridging ligand,  $\{[\text{Cu}_2(\mu\text{-ade})_4(\text{H}_2\text{O})_2][\text{Cu}(\text{ox})(\text{H}_2\text{O})]_2 \cdot \sim 14\text{H}_2\text{O}\}_n$  (**1**), has been synthesized by reaction of adenine (Hade) with a basic solution of  $\text{K}_2[\text{Cu}(\text{ox})_2] \cdot 2\text{H}_2\text{O}$  (ox = oxalato dianion). Compound **1** crystallizes in the trigonal space group  $R\bar{3}$  with  $a = b = 31.350(1)$  Å,  $c = 14.285(1)$  Å,  $V = 12158.7(10)$  Å<sup>3</sup>, and  $Z = 9$ . X-ray analysis shows a covalent 3D network in which the copper(II) centers are bridged by tridentate  $\mu\text{-N3,N7,N9}$  adeninate ligands. The compound has relatively large, nanometer-sized tubes associated with the self-assembly process directed solely by metal–ligand interactions. The covalent 3D framework remains intact upon removal of the guest water molecules trapped in the nanotubes. Magnetic measurements indicate an overall antiferromagnetic behavior of the compound.

Crystal engineering of high-dimensional frameworks from the self-assembly of transition metal complexes is one of the most challenging issues in current synthetic chemistry,<sup>1</sup> not only because of their intrinsic aesthetic appeal but also because of their potentially exploitable properties.<sup>2,3</sup> Previous studies have demonstrated that the most efficient approach to construct this type of material is to use the covalent linkages provided by multidentate organic ligands<sup>4</sup> and/or to utilize the hydrogen bonding and  $\pi\text{--}\pi$  stacking capabilities of suitable multifunctional ligands.<sup>5</sup> The judicious choice of the organic ligands is a key step in designing multidimensional framework compounds containing transition metal complexes as building blocks.

The unsubstituted adenine nucleobase contains at least five donor sites (N9, N7, N3, N1, and N10) capable of coordinat-

ing metallic ions, and its versatility as a ligand is well-known. The crystal structures of nearly 60 adenine transition metal complexes have been retrieved from the Cambridge structural database (CSD, Jan 2004 release),<sup>6</sup> and 11 different metal–ion binding patterns have been found.<sup>7</sup> Transition metal complexes containing nucleobases have been extensively studied as biomimetic systems<sup>8</sup> with the aim of analyzing the role of the noncovalent interactions (hydrogen bonds and  $\pi\text{--}\pi$  stackings) that are operative in the conformation and function of macromolecular biological systems. These complexes have also been used to investigate the DNA–metal binding processes that are essential in the development of new biologically active metallodrugs.<sup>9</sup>

Most of these compounds are monomers or discrete polymeric species of low nuclearity in which the supramolecular 3D structure is achieved by means of noncovalent interactions.<sup>8,10</sup> The number of  $n$ -dimensional ( $n\text{D}$ ,  $n = 1\text{--}3$ ) coordination polymers based only on the covalent interactions of a purine nucleobase is small. To our knowledge, this field is limited to some 1D complexes containing purine as terminal<sup>11</sup> or bridging ligands.<sup>12</sup>

We report herein the synthesis, crystal structure, thermal behavior, and magnetic properties of the first example of a covalent 3D network containing adenine as a bridging ligand, the porous coordination polymer  $\{[\text{Cu}_2(\mu\text{-ade})_4(\text{H}_2\text{O})_2][\text{Cu}(\text{ox})(\text{H}_2\text{O})]_2 \cdot \sim 14\text{H}_2\text{O}\}_n$  (**1**).<sup>13</sup>

The X-ray crystal structure analysis<sup>14</sup> revealed the presence of a unique 3D framework with two distinct types of neutral building blocks: dimeric  $[\text{Cu}_2(\mu\text{-ade})_4(\text{H}_2\text{O})_2]$  units and mononuclear  $[\text{Cu}(\text{ox})(\text{H}_2\text{O})]$  entities. A perspective view of

\* To whom correspondence should be addressed. E-mail: qipcacao@lg.ehu.es (O.C.), qipluara@lg.ehu.es (A.L.). Fax: +34 944 64 85 00.

- (1) (a) Moulton, B.; Zaworotko, M. J. *Chem. Rev.* **2001**, *101*, 1629. (b) James, S. L. *Chem. Soc. Rev.* **2003**, *32*, 276.
- (2) Janiak, C. J. *Chem. Soc., Dalton Trans.* **2003**, 2781.
- (3) Braga, D.; Desiraju, G. R.; Miller, J. S.; Orpen, A. G.; Price, S. L. *CrystEngComm* **2002**, *4*, 500.
- (4) Beobide, G.; Castillo, O.; Luque, A.; García-Couceiro, U.; García-Terán, J. P.; Román, P.; Lezama, L. *Inorg. Chem. Commun.* **2003**, *6*, 1224.

- (5) (a) Beatty, A. M. *CrystEngComm* **2001**, *51*, 1. (b) Roesky, H. W.; Andruh, M. *Coord. Chem. Rev.* **2003**, *236*, 91.
- (6) Allen, F. H. *Acta Crystallogr.* **2002**, *B58*, 380.
- (7) Abdus, M.; Aoki, K. *Inorg. Chim. Acta* **2000**, *311*, 15.
- (8) Lippert, B. *Coord. Chem. Rev.* **2000**, *200–202*, 487.
- (9) Berners-Price, S. J.; Sadler, P. J. *Coord. Chem. Rev.* **1996**, *151*, 1.
- (10) (a) Price, C.; Shipman, A.; Rees, N. H.; Elsegood, M. R. J.; Edwards, A. J.; Clegg, W.; Houlton, A. *Chem. Eur. J.* **2001**, *7*, 1194. (b) Price, C.; Horrocks, B. R.; Mayeux, A.; Elsegood, M. R. J.; Clegg, W.; Houlton, A. *Angew. Chem., Int. Ed.* **2002**, *41*, 1047.
- (11) (a) Sheldrick, W. S. *Acta Crystallogr.* **1981**, *B37*, 945. (b) Sletten, E.; Sletten, J.; Froystein, N. A. *Acta Chem. Scand.* **1988**, *A42*, 413.
- (12) Vestues, P. I.; Sletten, E. *Inorg. Chim. Acta* **1981**, *52*, 269.

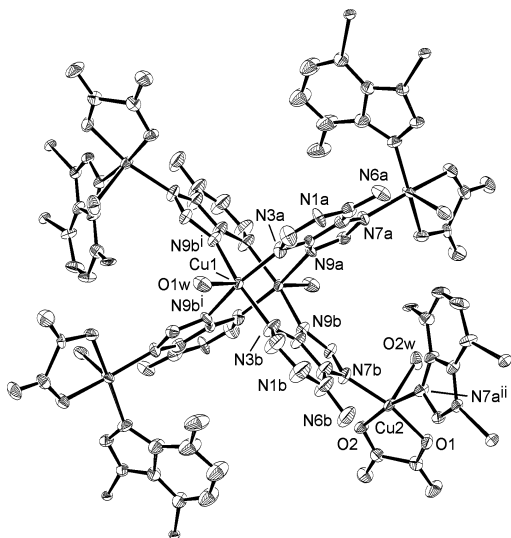


**Figure 1.** ORTEP view of a fragment of the polymeric network of **1** (30% probability thermal ellipsoids). H atoms are omitted for clarity. Selected bond distances (Å): Cu1–N3a, 2.000(8); Cu1–N9a<sup>i</sup>, 2.013(7); Cu1–N3b, 2.014(8); Cu1–N9b<sup>i</sup>, 2.003(7); Cu1–O1w, 2.172(6); Cu2–O1, 1.953(6); Cu2–O2, 1.930(6); Cu2–N7a<sup>ii</sup>, 1.985(7); Cu2–N7b, 1.997(7); Cu2–O2w, 2.317(7). Symmetry codes: (i)  $-x + 1, -y, -z$ ; (ii)  $-y + 1/3, x - y - 1/3, z - 1/3$ .

a fragment of the polymeric structure is given in Figure 1, together with selected bond lengths. The labeling scheme used here for the nucleobase is that conventionally accepted for chemical and biological purposes.

The dimeric fragment is centrosymmetric and is made of two Cu(II) atoms bridged by four adeninate anions in a windmill-shaped arrangement with a Cu1...Cu1<sup>i</sup> distance of 2.938(2) Å. The dihedral angle between the mean plane of the two crystallographically independent bridges (a and b) is 76.5(2)°. The basal positions of the distorted square-pyramidal coordination around the Cu(1) atom are occupied by two imidazole N9x atoms and two pyrimidinic N3x atoms of the deprotonated adeninate ligands with regular Cu–N bond distances of about 2.00 Å. The metal atom is displaced by 0.264(1) Å from this plane toward an apical coordinated water molecule at 2.172(6) Å. These structural parameters are similar to those reported for the dimeric compounds [Cu<sub>2</sub>(μ-Hade)<sub>4</sub>Cl<sub>2</sub>]Cl<sub>2</sub>·6H<sub>2</sub>O,<sup>15</sup> [Cu<sub>2</sub>(μ-Hade)<sub>4</sub>(H<sub>2</sub>O)<sub>2</sub>](ClO<sub>4</sub>)<sub>2</sub>·2H<sub>2</sub>O,<sup>16</sup> and [Cu<sub>2</sub>(μ-ade)<sub>4</sub>(H<sub>2</sub>O)<sub>2</sub>]·2H<sub>2</sub>O<sup>17</sup> containing μ-N3,N9 bridging ligands. Each dimeric fragment is linked to four neighboring monomeric entities via the N7x atom

from the imidazole ring of the adeninate ligands with bond distances of Cu2–N7a<sup>ii</sup> = 1.985(7) Å and Cu2–N7b = 1.997(7) Å.

Therefore, adeninate anions behave as tridentate μ-N3,N7,N9 bridging ligands. To our knowledge, this unusual coordination mode of the adenine has been reported only for some methylmercury(II) metalated adeninato(1–) derivatives,<sup>18</sup> but it has been also observed in some complexes of the immunosuppressant thiopurine drug azathioprine.<sup>19</sup> Another tridentate coordination mode (μ-1κN9:2κ<sup>2</sup>N6,N7) has been reported for the adeninate bridging ligand in organometallic tetrameric Cp\*Ir(III) and (*p*-cymene)Ru(II) complexes, but in these cases, the nucleobase is chelated to one metal by the imidazole N7 atom and the exocyclic N6 amino group to give a five-membered ring,<sup>20</sup> whereas in compound **1**, the amino groups remain uncoordinated and are hydrogen bonded to oxygen atoms.

The basal plane of the square-pyramidal chromophore around the Cu2 atom is completed by two oxygen atoms from a bidentate oxalato ligand. The Cu2 atom is displaced by 0.152(1) Å from the basal plane toward the apical water molecule at 2.317(7) Å. The Cu1...Cu2 distance [5.857(4) Å] is similar to those reported for the dimer [Cu<sub>2</sub>(NBzIDA)<sub>2</sub>-(μ-Hade)(H<sub>2</sub>O)<sub>2</sub>]·3H<sub>2</sub>O [5.926(1) Å, NBzIDA is the *N*-benzyliminodiacetato dianion]<sup>21</sup> and for the 1D complex {[Cu(μ-purine)(H<sub>2</sub>O)<sub>4</sub>]SO<sub>4</sub>·2H<sub>2</sub>O}<sub>n</sub> [5.956(1) Å]<sup>12</sup> in which the purine nucleobases show a similar bidentate μ-N7,N9 bridging coordination mode.

The self-assembly process directed by the metal–adeninate linkages creates nanotubular channels along the crystallographic *c* axis with a diameter of about 13 Å, as shown in Figure 2. Calculations using PLATON<sup>22</sup> showed that the effective volume for inclusion is greater than 4916 Å<sup>3</sup>/cell, comprising 40.4% of the crystal volume. Many guest water molecules are trapped in the parallel tubes.<sup>23</sup> The solvated water molecules are engaged themselves and anchored to

- (13) Dark-blue single crystals of **1** were grown by the slow diffusion of a methanolic solution (15 mL) of adenine (0.56 mmol) into a solution of K<sub>2</sub>[Cu(ox)<sub>2</sub>]·2H<sub>2</sub>O (0.12 mmol) in 20 mL of 0.2 M NaOH to deprotonate the nucleobase, which increases the number of potential donor sites. Yield 20% (based on metal). Anal. Calcd for C<sub>24</sub>H<sub>52</sub>Cu<sub>4</sub>N<sub>20</sub>O<sub>26</sub>: C, 22.33; H, 4.06; N, 21.70; Cu, 19.69. Found: C, 22.16; H, 4.00; N, 21.45; Cu, 19.33%.
- (14) Crystal data for **1**: crystal dimensions 0.16 × 0.08 × 0.06 mm, trigonal, R3̄; *a* = *b* = 31.350(1) Å, *c* = 14.285(1) Å, *V* = 12158.7(10) Å<sup>3</sup>, *Z* = 9, formula weight = 1290.98 g mol<sup>-1</sup>, *D*<sub>calc</sub> = 1.586 Mg·m<sup>-3</sup>, 2θ<sub>max</sub> = 60°, Xcalibur diffractometer, *T* = 293(2) K, λ(Mo Kα) = 0.71073 Å, μ = 1.643 mm<sup>-1</sup>, 40448 reflections, 7878 unique reflections, 310 parameters, R1(*F*<sub>o</sub>) = 0.0658 [*I* > 2σ(*I*)], wR2(*F*<sub>o</sub><sup>2</sup>) = 0.1663 (all data), GOF = 1.002, maximum residual electron density 0.741 e Å<sup>-3</sup>.
- (15) de Meester, P.; Skapski, A. C. *J. Chem. Soc.* **1971**, A13, 2167.
- (16) Terzis, A.; Beauchamp, A. L.; Rivest, R. *Inorg. Chem.* **1973**, 12, 1166.
- (17) Sletten, E. *Acta Crystallogr.* **1969**, B25, 1480.

- (18) (a) Hubert, J.; Beauchamp, A. L. *Can. J. Chem.* **1980**, 58, 1439. (b) Hubert, J.; Beauchamp, A. L. *Acta Crystallogr.* **1980**, B36, 2613. (c) Charland, J. P.; Britten, J. F.; Beauchamp, A. L. *Inorg. Chim. Acta* **1986**, 124, 161.
- (19) (a) Zhu, F. C.; Schmalte, H. W.; Fischer, B.; Dubler, E. *Inorg. Chem.* **1998**, 37, 1161. (b) Chifotides, H. T.; Katsaros, N.; Pneumatikakis, G. *J. Inorg. Biochem.* **1994**, 56, 249. (c) Chifotides, H. T.; Dunbar, K. R.; Katsaros, N.; Pneumatikakis, G. *J. Inorg. Biochem.* **1994**, 55, 203.
- (20) (a) Korn, S.; Sheldrick, W. S. *Inorg. Chim. Acta* **1997**, 254, 85. (b) Annen, P.; Schildberg, S.; Sheldrick, W. S. *Inorg. Chim. Acta* **2000**, 307, 115. (c) Fish, R. H.; Jaouen, G. *Organometallics* **2003**, 22, 2166.
- (21) Rojas-González, P. X.; Castiñeiras, A.; González-Pérez, J. M.; Choquesillo-Lazarte, D.; Niclós-Gutiérrez, J. *Inorg. Chem.* **2002**, 41, 6190.
- (22) Spek, A. L. *PLATON, A Multipurpose Crystallographic Tool*; Utrecht University: Utrecht, Holland, 1998.
- (23) After completing the initial structure solution, a difference Fourier map showed the presence of substantial electron density (maximum peak 1.95 e Å<sup>-3</sup>) spreading out around the crystallographic 3-fold screw axis at the center of the voids. No satisfactory model for the disorder could be found, and for further refinements, the contribution of the missing solvent molecules was subtracted from the reflection data by the SQUEEZE method (Van der Sluis, P.; Spek, A. L. *Acta Crystallogr.* **1990**, A46, 194) as implanted in PLATON. The final R1 [*I* > 2σ(*I*)] and wR2 values before SQUEEZE were 0.1148 and 0.2211, respectively. An accurate determination of the stoichiometric quantity of solvent was obtained from the TGA/DTA curves (see Supporting Information).

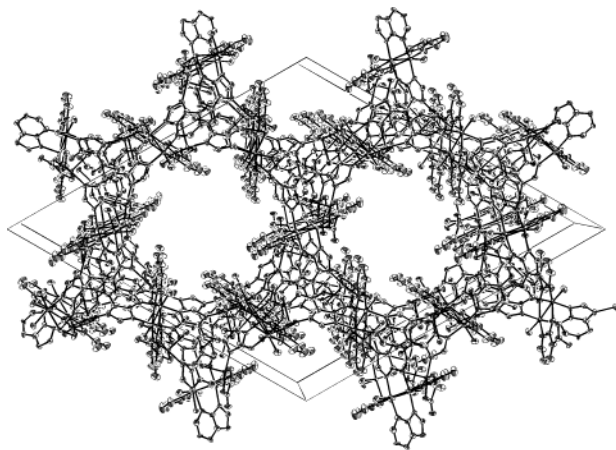


**Figure 2.** Perspective view of the 3D framework along the  $c$  axis, showing the nanopores. Solvated water molecules are omitted for clarity.

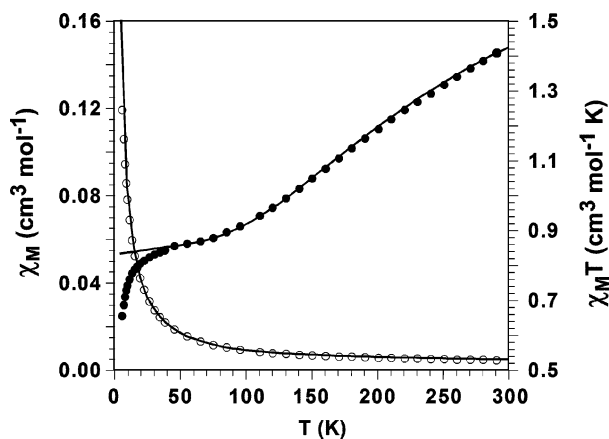


**Figure 3.** Thermal dependence of the  $\chi_M$  (○) and  $\chi_M T$  (●) curves for compound **1**. Continuous lines correspond to the best least-squares fit of the high-temperature data ( $T > 30$  K).

the inner walls of the nanotubes essentially via hydrogen bonds involving the coordinated water molecules, the uncoordinated oxygen oxalato atoms, and the amino groups of the adeninato bridges.

Thermal degradation of compound **1** starts with an initial well-separated weight loss of 18.6%, between 40 and 95 °C, corresponding to the loss of 14 solvated water molecules per formula unit (calcd 19.5%). The large crystals do not change their external morphology during their dehydration, and the XRPD pattern of hydrated and dehydrated samples of **1** do not differ substantially, suggesting that the 3D framework structure is maintained after the crystallization water molecules are removed (see Supporting Information).

Plots showing the thermal evolution of the magnetic molar susceptibility and the product  $\chi_M T$  are presented in Figure 3 ( $T$  range, 5–300 K; applied field, 1000 G). The room-temperature  $\chi_M T$  value ( $1.41 \text{ cm}^3 \text{mol}^{-1} \text{K}$ ) is lower than that expected for four uncoupled Cu(II) ions ( $1.50 \text{ cm}^3 \text{mol}^{-1} \text{K}$ , considering  $g = 2.00$ ) and decreases rapidly upon cooling to 70 K, reaching a plateau with a value of  $0.85 \text{ cm}^3 \text{mol}^{-1} \text{K}$ . Below 40 K, the curve decreases again to  $0.66 \text{ cm}^3 \text{mol}^{-1} \text{K}$ .

at 5 K, which is lower than the value corresponding to the presence of two uncoupled Cu(II) atoms ( $0.75 \text{ cm}^3 \text{mol}^{-1} \text{K}$ ,  $g = 2.00$ ). A priori, the magnetic behavior of this compound must be dominated by the presence of two magnetic exchange pathways, one resulting from the four Cu1–N3–C4–N9–Cu1<sup>I</sup> bridges in the dimeric core and the other from the imidazole bridges that link the dimeric and four adjacent monomeric entities. For the first pathway, singlet–triplet energy gap ( $J$ ) values near  $-300 \text{ cm}^{-1}$  have been reported for the complexes  $[\text{Cu}_2(\mu\text{-Hade})_4\text{Cl}_2]\text{Cl}_2 \cdot 6\text{H}_2\text{O}$ ,<sup>15,24</sup>  $[\text{Cu}_2(\mu\text{-Hade})_4(\text{H}_2\text{O})_2](\text{ClO}_4)_2 \cdot 2\text{H}_2\text{O}$ ,<sup>16,25</sup> and  $[\text{Cu}_2(\mu\text{-ade})_4(\text{H}_2\text{O})_2] \cdot 2\text{H}_2\text{O}$ .<sup>17</sup> With respect to the superexchange magnetic coupling through bidentate  $\mu\text{-N7,N9}$  purine nucleobases, to date, the available magnetic data for complexes based on this type of bridge indicate very weak antiferromagnetic coupling between the Cu(II) ions.<sup>21,26</sup>

From a structural viewpoint, the title compound exhibits a 3D framework, but keeping in mind the capacity of the bridges to transmit magnetic interactions and the overall appearance of the  $\chi_M T$  curve, we tried to fit the experimental magnetic data by using the Bleaney–Bowers equation ( $H = -JS_1S_2$ ) for a dinuclear copper(II) complex,<sup>27</sup> modified to take into account the presence of one dimeric and two monomeric copper entities per formula unit. No reasonable fit could be obtained over the whole experimental curve, but by taking into account only the data above 30 K, a relatively good fit could be achieved (solid lines in Figure 3) with the parameters  $J = -316 \text{ cm}^{-1}$ ,  $g_d = 2.11$ , and  $g_m = 2.10$ .  $g_d$  and  $g_m$  are the mean  $g$  factors for the copper(II) ions of the dimeric and monomeric fragments, respectively. Even if the fit is not completely satisfactory, the calculated  $J$  value is in good agreement with the structural characteristics, and it can be considered as a rather good approximation. The discrepancy between experimental and calculated data at lower temperatures suggests that the participation of the imidazole bridges in the magnetic exchange between the dimeric (Cu1) and monomeric (Cu2) entities cannot be a priori disregarded.

**Acknowledgment.** This work was supported by the Spanish Ministerio de Ciencia y Tecnología (MAT2002-03166) and the Universidad del País Vasco/Euskal Herriko Unibertsitatea (9/UPV 00169.310-15329/2003). J.P.G.-T. and U.G.-C. thank these institutions for predoctoral fellowships.

**Supporting Information Available:** X-ray crystallographic file in CIF format, FT-IR spectra, TGA/DTA curves, variable-temperature XRPD patterns, and ORTEP views. This material is available free of charge via the Internet at <http://pubs.acs.org>.

IC049512V

- (24) Curran, R. T.; Villa, J. F. *Proc. 16th Int. Conf. Coord. Chem.* **1974**, *2.21a*, 3.  
 (25) Hanson, M. V.; Smith, C. B.; Simpson, G. D.; Carlisle, G. O. *Inorg. Nucl. Chem. Lett.* **1975**, *11*, 225.  
 (26) Salam, M. A.; Aoki, K. *Inorg. Chim. Acta* **2001**, *314*, 71.  
 (27) Bleaney, B.; Bowers, K. D. *Proc. R. Soc. London, Ser. A* **1952**, *214*, 451.